Human Molecular Genetics, 2004, Vol. 13, No. 7 ***669–681***
DOI: 10.1093/hmg/ddh082
Advance Access published on February 12, 2004

Striatal cells from mutant huntingtin knock-in mice are selectively vulnerable to mitochondrial complex II inhibitor-induced cell death through a non-apoptotic pathway

Qingmin Ruan[1], Mathieu Lesort[1], Marcy E. MacDonald[2] and Gail V.W. Johnson[1,*]

[1]Department of Psychiatry, 1720 7th Avenue South, SC 1061, University of Alabama at Birmingham, Birmingham, AL 35294-0017, USA and [2]Molecular Neurogenetics Unit, Massachusetts General Hospital, Building 149, 13th Street, Charlestown, MA 02129, USA

Received October 2, 2003; Revised and Accepted January 30, 2004

Extensive striatal neuronal loss occurs in Huntington's disease (HD), which is caused by an expanded polyglutamine tract in huntingtin (htt). Evidence suggests that mutant htt directly or indirectly compromises mitochondrial function, contributing to the neuronal loss. To determine the role of compromised mitochondrial function in the neuronal cell death in HD, immortalized striatal cells established from Hdh^{Q7} (wild-type) and Hdh^{Q111} (mutant) mouse knock-in embryos were treated with 3-nitropropionic acid (3-NP), a mitochondrial complex II toxin. 3-NP treatment caused significantly greater cell death in mutant striatal cells compared with wild-type cells. In contrast, the extent of cell death induced by rotenone, a complex I inhibitor, was similar in both cell lines. Although evidence of apoptosis was present in 3-NP-treated wild-type striatal cells, it was absent in 3-NP-treated mutant cells. 3-NP treatment caused a greater loss of mitochondrial membrane potential ($\Delta\psi m$) in mutant striatal cells compared with wild-type cells. Cyclosporine A, an inhibitor of mitochondrial permeability transition pore (PTP), and ruthenium red, an inhibitor of the mitochondrial calcium uniporter, both rescued mutant striatal cells from 3-NP-induced cell death and prevented the loss of $\Delta\psi m$. These data show that mutant htt specifically increases cell vulnerability to mitochondrial complex II inhibition and further switched the type of cell death induced by complex II inhibition from apoptosis to a non-apoptotic form, caused by mitochondrial membrane depolarization, probably initiated by mitochondrial calcium overload and subsequent PTP opening. These findings suggest that impaired mitochondrial complex II function in HD may contribute to non-apoptotic neuronal cell death.

INTRODUCTION

Huntington's disease (HD) is a dominantly inherited disorder characterized by a progressive loss of neurons in the striatum (1). The mutation causing HD is a CAG repeat expansion in the gene encoding huntingtin (htt) (2).

The pathogenic mechanisms by which mutant htt causes neuronal cell death remain uncertain. Although htt is expressed ubiquitously (3,4), the striatum is most affected in HD (1,5). Further, it is unclear whether neurons die by apoptotic or non-apoptotic processes. Markers of apoptosis have been found in HD postmortem brain and in the R6/2 transgenic HD mouse model (6), and treatment with caspase inhibitors or the use of dominant negative caspase 1 slowed disease progression in R6/2 mice (7,8). On the other hand, overexpression of dominant-negative caspase-1 in HD knock-in mice failed to alter the timing of early disease events (9). Further, in knock-in mouse models of HD, evidence of apoptosis is absent (10,11).

Mitochondria play an important role in both apoptotic and non-apoptotic cell death (12). In apoptosis, the release of cytochrome c from mitochondria initiates a caspase-dependent apoptotic cascade (13–16). Non-apoptotic cell death is mainly associated with the loss of mitochondrial membrane potential ($\Delta\psi m$) (12). Loss of $\Delta\psi m$ can be due to permeability transition pore (PTP) opening (17), and mitochondrial calcium overload is an important factor in PTP opening (18). Interestingly, in terms of specific mitochondrial changes, there is no distinct boundary between apoptotic and non-apoptotic cell death. For example,

*To whom correspondence should be addressed. Tel: +1 2059342465; Fax: +1 2059343709; Email: gvwj@uab.edu

mitochondrial membrane depolarization occurs in many apoptotic cell death models (19,20), while in non-apoptotic cell death, cytochrome c release is not uncommon (21).

One proposed mechanism for the selective neuronal loss in HD is mitochondrial dysfunction. In HD abnormalities in mitochondrial oxidative metabolism exist (22) and increased stress-induced mitochondrial depolarization is observed (23). Selective decreases in the activity of mitochondrial complex II and III in the striatum of HD cases have been reported (24,25). Interestingly, no deficiencies in the activity of mitochondrial respiratory chain enzymes were observed in brain regions relatively spared in HD (25) and in platelets from HD cases (24). These findings suggest that the selective impair of mitochondrial respiratory function in the striatum may play a role in the pathogenesis of HD. Mitochondrial complex II inhibitors such as 3-nitropropionic acid (3-NP) or malonate have been found useful in producing animal models of HD (26–28). These data further support the hypothesis that deficits in mitochondrial complex II may play a role in the specific vulnerability of striatum in HD. Mitochondrial calcium abnormalities occur early in HD and may also contribute to the pathogenic cascade in HD (29). *In vitro*, polyglutamine constructs can directly promote mitochondrial deenergization during graded calcium load (30).

Given these previous findings the goal of this study was to determine the consequences of compromised mitochondrial function in immortalized striatal cells that were established from $Hdh^{Q7/Q7}$ (wild-type) and homozygous mutant $Hdh^{Q111/Q111}$ knock-in mouse embryos (31). We demonstrate that although mitochondrial complex II inhibition results in apoptotic cell death in wild-type striatal cells, mutant striatal cells die by a non-apoptotic process involving mitochondrial calcium overload, PTP opening and mitochondrial membrane depolarization.

RESULTS

Mutant htt specifically increases cell vulnerability to a mitochondrial complex II inhibitor

To determine if mutant htt selectively sensitizes cells to mitochondrial complex II inhibition, human SH-SY5Y neuroblastoma cell lines stably overexpressing htt with 23 (FL-Q23) or 82 (FL-Q82) glutamine repeats were treated with 3-NP, an irreversible mitochondrial complex II inhibitor (32). Treatment with 3-NP resulted in a significantly greater increase in cell death in FL-Q82 cells than in FL-Q23 cells (Fig. 1A). When FL-Q23 and FL-Q82 cells were treated with rotenone, a mitochondrial complex I inhibitor, there was no significant difference in cell death between these two cell lines (Fig. 1B). Under basal conditions, no significant difference in the extent of cell death was observed between these two cell lines. These findings clearly indicate that the expression of mutant htt selectively potentiated the inhibition of complex II-induced cell death.

To further determine if mutant htt has the same effect when it is expressed at endogenous levels and in an HD-appropriate neuronal context, conditionally immortalized wild-type and mutant striatal cells were incubated in the absence or presence of 3-NP prior to the measurement of cell death. These cells display characteristics of medium spiny neurons, which are most vulnerable in HD, and therefore are an appropriate HD cell model (31). In the absence of 3-NP the extent of LDH release was not significantly different between wild-type and mutant striatal cells (Fig. 2A). A previous study had shown that under basal conditions MTT reduction to formazan was significantly less in mutant striatal cells compared with wild-type cells (33). However, the MTT assay is a general measure of the reducing capacity of the cell (both mitochondrial and non-mitochondrial) (34) and not a direct indicator of cell viability. Treatment with 3-NP resulted in a dose-dependent increase in the percent of LDH released, indicating increased cell death. However, cell death in mutant striatal cells was significantly greater than that in wild-type striatal cells in response to 3-NP treatment (Fig. 2A). Similar results were obtained when another cell death measurement, calcein AM uptake, was used (Fig. 2B). Cell survival was also determined by cell counts and in agreement with the previous measures, revealed a significant decrease in the survival of 3-NP treated mutant cells, compared with their wild-type counterparts (Fig. 2C). These findings are also in agreement with a previous report showing that 3-NP-treatment resulted in greater cell loss in mutant striatal cells compared with wild-type cells (33). In contrast, there was no difference in the extent of cell death when wild-type and mutant striatal cells were treated with rotenone, a mitochondrial complex I inhibitor (Fig. 2D). Thus, in two different cellular models, mutant htt selectively potentiated cell death induced by inhibition of complex II activity; however, given the fact that the immortalized striatal cells represent a more accurate HD model system, all subsequent experiments were carried out using these cell lines.

3-NP treatment results in apoptotic chromatin condensation only in wild-type striatal cells

The striatum is the primary area of neuronal degeneration in HD (5) and the mechanism of this selective pattern of neurodegeneration is not clear. Despite substantial evidence from *in vitro* studies that connects mutant htt with the neuronal death in HD, evidence of apoptosis in HD cases and in mouse models of HD remains limited. Indeed, a non-apoptotic neurodegenerative pathway has been proposed (35,36). Therefore we next investigated if there was evidence of apoptosis in wild-type and/or mutant striatal cells treated with 3-NP. Cells were incubated in the absence or presence of 3-NP and then stained with DAPI to visualize chromatin condensation, a characteristic change in apoptosis. As expected, there were no apoptotic nuclei in either wild-type or mutant striatal cells under control conditions (Fig. 3). In contrast, incubation of the wild-type striatal cells with 3-NP resulted in the presence of prominent apoptotic nuclear condensation, which was not detected in the mutant striatal cells (Fig. 3). Given the fact that 3-NP treatment results in a higher rate of cell death in mutant striatal cells compared with wild-type cells (Fig. 2), these data suggest that 3-NP treatment of mutant striatal cells results in non-apoptotic cell death.

3-NP treatment results in cytochrome c release in wild-type striatal cells but not in mutant striatal cells

Cytochrome c released to the cytosol initiates the mitochondria-dependent apoptotic pathway (37,38). To further determine

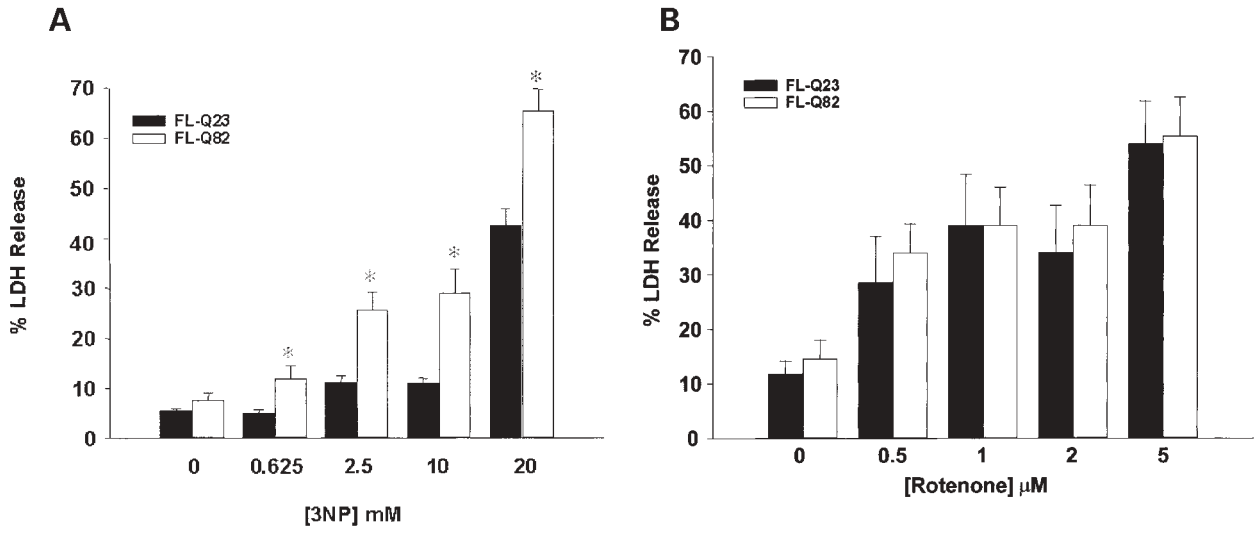

Figure 1. SH-SY5Y cells overexpressing mutant htt are selectively vulnerable to 3-NP. (**A**) FL-Q23 and FL-Q82 cells were treated with 3-NP for 16 h, and cell death was measured by LDH release. LDH release in FL-Q82 cells was significantly greater than that in FL-Q23 cells at the indicated 3-NP concentrations. Mean ± SEM, $n = 3$, $^*P < 0.05$. (**B**) FL-Q23 and FL-Q82 cells were treated with rotenone for 16 h, and cell death was measured by LDH release. There was no significant difference in LDH release in response to rotenone between these two cell lines. Mean ± SEM, $n = 3$.

whether cell death induced by complex II inhibition is apoptotic, wild-type and mutant striatal cells were incubated in the absence or presence of 3-NP prior to isolating cytosolic and mitochondrial fractions and probing for cytochrome c. No cytochrome c was detected in the cytosol in either cell line under control conditions (Fig. 4). However, in the wild-type striatal cells 3-NP treatment increased cytochrome c levels in the cytosol with a concomitant decrease of cytochrome c in the mitochondrial fraction. In contrast, no cytochrome c release was detected in the 3-NP treated mutant striatal cells (Fig. 4).

3-NP treatment results in caspase-9 activation, caspase-3 activation and PARP cleavage in wild-type striatal cells but not in mutant striatal cells

Release of cytochrome c from the mitochondria results in the processing of pro-caspase-9 into its active fragment (13). Active caspase-9 subsequently converts pro-caspase-3 into its active form (14,15), which in turn cleaves a set of cellular substrates, including PARP (39), a DNA repair enzyme (16). Therefore we next investigated whether 3-NP treatment resulted in downstream events in the apoptotic cascade, such as caspase activation and PARP cleavage. Wild-type and mutant striatal cells were incubated in the absence or presence of 3-NP prior to collecting and immunoblotting for the pro-form of caspase-9, active caspase-3 or cleaved PARP. In the absence of 3-NP no active caspase-3 or cleaved PARP was detected in either cell line (Fig. 5A). Incubation of the wild-type striatal cells with 3-NP resulted in the presence of active caspase-3 and cleaved PARP, and a decrease in the levels of the pro-form of caspase-9, indicating that caspase-9 was activated (Fig. 5A). In contrast, when mutant striatal cells were incubated with 3-NP under identical conditions, no increase in the levels of active caspase-3 or cleaved PARP was observed and there was no change in the levels of the pro-form of caspase-9 (Fig. 5A).

Caspase-3 activity was also quantitatively measured in wild-type and mutant striatal cells incubated in the absence or presence of 3-NP. These results revealed that 3-NP treatment resulted in a significant increase in caspase-3 activity in wild-type striatal cells, while no increase was observed in mutant striatal cells (Fig. 5B). Given the possibility that 3-NP-induced capase-3 activation may occur earlier in the mutant striatal cells than in the wild-type striatal cells, caspase-3 activity was also measured at 5, 14 and 24 h after addition of 3-NP. No 3-NP-induced increase in caspase-3 activity was observed in the mutant striatal cells at any of these time points (data not shown). Taken together, all these results clearly demonstrate that the cell death induced by 3-NP in mutant striatal cells is non-apoptotic in contrast to the apoptotic cell death that occurs in wild-type striatal cells.

To further determine the contribution of the apoptotic pathway to the 3-NP-induced cell death, wild-type and mutant striatal cells were incubated with 3-NP in the absence or presence of Boc-D(Ome)-FMK (BAF), a broad-spectrum caspase inhibitor (40), prior to the measurement of cell viability. BAF pre-treatment significantly decreased 3-NP-induced cell death in wild-type striatal cells, but had no effect on 3-NP induced cell death in mutant striatal cells (data not shown).

3-NP treatment results in a greater decrease in $\Delta\psi m$ in mutant striatal cells compared to wild-type striatal cells

Mitochondrial membrane depolarization can result in cell death (41,42) and is suggested to be involved in selective neuronal death in HD (29). To investigate whether inhibition of complex II results in mitochondrial depolarization, wild-type and mutant striatal cells were incubated in the absence or presence 3-NP and $\Delta\psi m$ was measured with JC-1. Under control conditions, both wild-type (Fig. 6A) and mutant (Fig. 6B) striatal cells exhibit red JC-1 aggregates, indicative of a relatively high

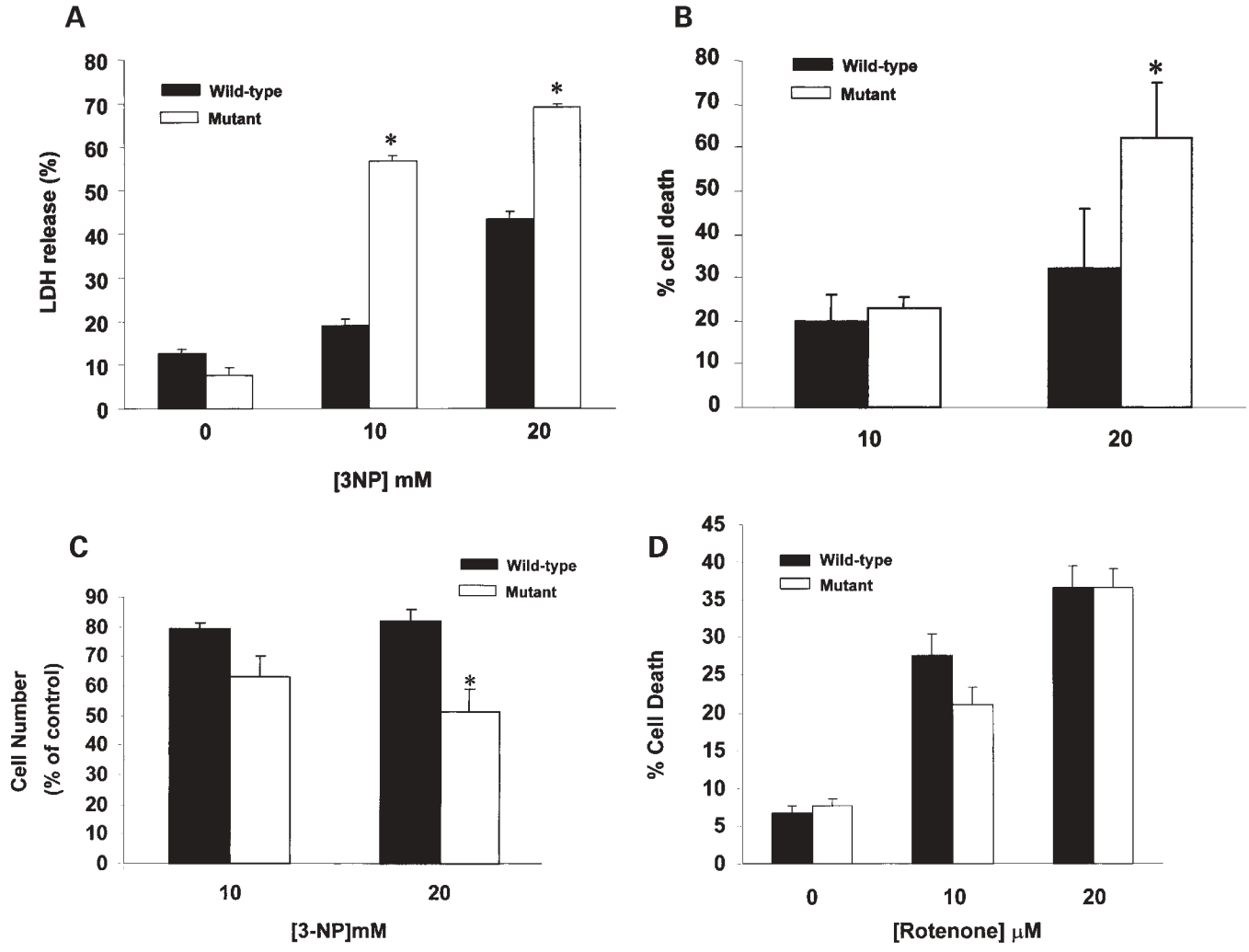

Figure 2. Striatal cells expressing mutant htt are selectively vulnerable to 3-NP. (**A**) Wild-type and mutant striatal cells were treated with 3-NP for 40 h, and cell death was measured by LDH release. LDH release in mutant striatal cells was significantly greater than in wild-type striatal cells. Mean ± SEM, $n = 3$, $^*P < 0.05$ when comparing LDH release between these two cell lines at 10 and 20 mM 3-NP. (**B**) Wild-type and mutant striatal cells were treated with 3-NP for 40 h, and cell death was measured by calcein-AM. Cell death in mutant striatal cells was significantly greater than in wild-type striatal cells with 20 mM 3-NP. Mean ± SEM, $n = 3$, $^*P < 0.05$ when comparing cell death between these two cell lines. (**C**) Wild-type and mutant striatal cells were incubated in the absence or presence of 3-NP for 40 h, then stained with DAPI and cell number was determined. The number of surviving mutant striatal cells was significantly lower than that of wild-type striatal cells in response to 20 mM 3-NP treatment. Data is expressed as the proportion of cells present in the 3-NP treated wells, relative to parallel untreated wells. Mean ± SEM, $n = 3$, $^*P < 0.05$ when comparing the percentage of surviving cells between these two cell lines. (**D**) Wild-type and mutant striatal cells were treated with rotenone for 20 h, and cell death was measured using calcein-AM. There was no significant difference in cell death between these two cell lines in response to rotenone. Mean ± SEM, $n = 3$.

$\Delta\psi$m. In the wild-type striatal cells (Fig. 6A), treatment with 3-NP did not noticeably reduce the presence of the red JC-1 aggregates. In contrast, in mutant striatal cells, 3-NP treatment resulted in a dramatic decrease of red JC-1 aggregates (Fig. 6B), indicating that the mitochondria are depolarized. Further, we took advantage of the fact that the ratio of JC-1 aggregates to monomers staining is independent of cell number or mitochondrial density to quantitatively measure changes in $\Delta\psi$m (43) in wild-type and mutant cell lines that were incubated in the absence or presence of 3-NP. Quantitated data revealed that 3-NP treatment resulted in only a moderate decrease of $\Delta\psi$m in wild-type striatal cells (Fig. 6C), and further the decrease of $\Delta\psi$m was similar in cells incubated with 10 or 20 mM 3-NP, suggesting that wild-type striatal cells are able to maintain their $\Delta\psi$m. In contrast, 3-NP treatment of mutant striatal cells resulted in a significant and dose-dependent decrease of the $\Delta\psi$m (Fig. 6C).

Inhibition of mitochondrial Ca^{2+} influx reduces 3-NP-induced cell death in mutant and wild-type striatal cells

Several studies have suggested calcium disturbances are involved in the pathophysiological mechanisms of HD (44,45), and mitochondrial calcium overload, which leads to mitochondrial membrane depolarization is believed to cause

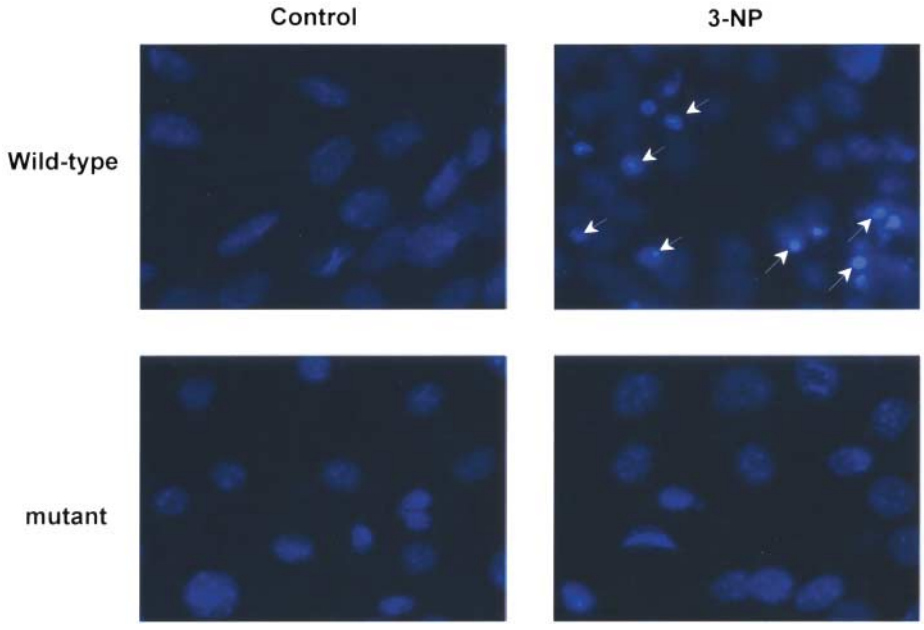

Figure 3. 3-NP causes apoptotic chromatin condensation only in wild-type striatal cells. Wild-type and mutant striatal cells were incubated under control conditions, or in the presence of 10 mM 3-NP for 40 h and cell nuclei were stained with DAPI to detect the presence of apoptotic chromatin condensation. Only wild-type striatal cells showed distinctive apoptotic nuclei condensation. Arrows indicate representative apoptotic chromatin condensation.

the opening of the PTP (46). To investigate the putative role of the mitochondrial calcium influx in the neuronal cell death induced by complex II inhibition, wild-type and mutant striatal cells were treated with 3-NP in the absence or presence of ruthenium red, an effective inhibitor of the mitochondrial Ca^{2+} uniporter (47), prior to the measurement of cell death. Ruthenium red significantly decreased cell death in 3-NP-treated mutant striatal cells (Fig. 7A). Although ruthenium red also reduced cell death in the 3-NP treated wild-type cells, it was to a much lesser extent than what was observed in the mutant striatal cells (Fig. 7A). We next examined whether ruthenium red rescued cells from death by preventing the 3-NP-induced mitochondrial depolarization by using JC-1. Quantitated data revealed that ruthenium red treatment prevented the 3-NP-induced decrease of JC-1 ratio in mutant striatal cells (Fig. 7B). Although ruthenium red also had an effect in wild-type striatal cells, it was to a much lesser extent than what was observed in the mutant striatal cells (Fig. 7B). These findings demonstrate that inhibiting mitochondrial calcium influx prevented the 3-NP-induced mitochondrial depolarization.

Inhibition of permeability transition pore (PTP) rescued 3-NP-induced cell death in mutant striatal cell

3-NP treatment results in mitochondrial membrane depolarization in mutant striatal cells (Fig. 6). Mitochondrial depolarization during cell death has been reported to be partially due to the opening of the PTP (48). To test whether the opening of the PTP contributed to 3-NP-induced cell death, wild-type and mutant striatal cells were treated with 3-NP with or without co-incubation with cyclosporine A (CsA), an inhibitor of PTP (49), prior to the measurement of cell death. CsA significantly decreased cell death in 3-NP treated mutant, but not wild-type striatal cells (Fig. 8A).

We next examined whether CsA rescued cells from death by preventing the 3-NP-induced decrease in $\Delta\psi m$. Wild-type and mutant striatal cells were treated with 3-NP in the absence or presence of CsA, prior to incubation with JC-1 to detect changes in $\Delta\psi m$. Quantitated data revealed that CsA treatment prevented the 3-NP-induced decrease of JC-1 ratio in mutant striatal cells but not wild-type striatal cells (Fig. 8B). The effects of CsA on 3-NP-induced cytochrome c release were also examined. Wild-type and mutant striatal cells were treated with 3-NP in the absence or presence of CsA, and then cytosolic fractions were isolated and probed for cytochrome c. In the wild-type striatal cells, CsA treatment did not prevent cytochrome c release induced by 3-NP, while in mutant striatal cells no cytosolic cytochrome c was detected under any condition (Fig. 8C).

DISCUSSION

The results of this study demonstrate that striatal cells derived from a precise genetic mouse model for HD are selectively vulnerable to mitochondrial complex II inhibition resulting in non-apoptotic cell death. Inhibition of mitochondrial PTP by CsA, and blockade of the calcium uniporter by ruthenium red, both protected mutant striatal cells from the 3-NP-induced toxicity. Further the 3-NP-induced loss of $\Delta\psi m$, which occurred primarily in the mutant striatal cells, was ameliorated by both ruthenium red and CsA treatment. Taken together these results indicate that mutant htt facilitates cell death by reducing the threshold for calcium-mediated opening of the mitochondria PTP.

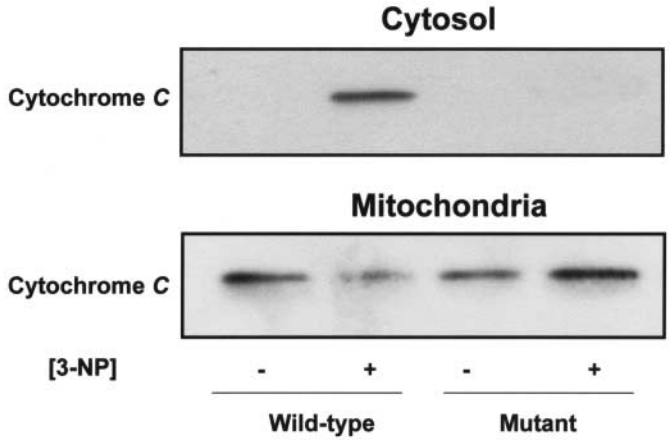

Figure 4. 3-NP treatment results in cytochrome c release in wild-type striatal cells but not in mutant striatal cells. Cells were incubated under control conditions (−), or in the presence of 10 mM 3-NP (+) for 40 h. Cytosolic and mitochondrial fractions were isolated and were probed for cytochrome c. No cytochrome c was present in the cytosol in either cells line under control conditions. However, in the wild-type striatal cells, cytochrome c re-located to cytosol after 3-NP treatment, while it was not detected in the cytosolic fraction of the 3-NP treated mutant striatal cells. Immunoblots shown are representative of three to six independent experiments.

Both overexpression of mutant htt in human neuroblastoma cells and expression of mutant htt at endogenous levels in striatal cells resulted in selective vulnerability to a mitochondrial complex II inhibitor (3-NP), but not a complex I inhibitor (rotenone). These findings are in agreement with a previous study that showed 3-NP treatment resulted in a greater cell death in mutant striatal cells compared with wild-type striatal cells (33). These results suggest that mutant htt specifically impairs the functioning of mitochondrial complex II. However, reports have indicated that the R6/2 mouse model of HD shows both increased (50) and decreased (51) resistance to 3-NP-induced striatal toxicity. Although the reasons for the discrepancies between these two studies is unclear, it should be noted the R6/2 mice overexpress exon 1 of the htt gene with ∼150 glutamine repeats (52), in contrast to the model system used in this study where the striatal cells were derived from a mutant htt knock-in mouse (53), a more precise genetic HD model system. Therefore, it can be suggested that expression of the mutant protein at physiological relevant levels provides a more appropriate model system to evaluate alterations in metabolic processes. In this study we provide convincing evidence that mutant htt specifically increases vulnerability to 3-NP. The mechanism by which mutant htt compromises the function of complex II has not yet been established. Interestingly, several genes that encode for mitochondrial metabolic proteins were among those that were decreased in HD mouse models (54–56). Therefore, it can be hypothesized that mutant htt, by affecting the transcriptional regulation of specific genes, may impact the expression and/or function of one of the four subunits of mitochondrial complex II (57), proteins involved in moving the subunits through the cytosol and targeting them to the mitochondria for import and/or the proteins that are involved in folding the catalytic subunits in the mitochondrial matrix (58,59). In addition to affecting transcriptional processes, mutant htt could also directly affect protein transport (60,61) and/or mitochondrial protein import processes (29,30) that could impact complex II function. Further research is required to elucidate the exact mechanism by which mutant htt selectively impairs mitochondrial complex II activity in HD.

In the present study inhibition of complex II resulted in significantly greater cell death and mitochondrial membrane depolarization in mutant striatal cells than that in wild-type cells. The 3-NP-induced cell death in the mutant striatal cells was non-apoptotic as evidenced by the fact that there was no cytochrome c release or caspase activation and BAF, a potent caspase inhibitor, failed to prevent the 3-NP-induced cell death. Apoptosis can also be caspase independent, due to apoptosis inducing factor (AIF) being released from the mitochondria and relocating into the nuclei (62). However no 3-NP-induced AIF nuclear translocation was observed in either cell line (data not shown). Together, these results show that death of the mutant striatal cells induced by mitochondrial complex II inhibition is non-apoptotic. Treatment with thapsigargin, an inhibitor of endoplasmic reticulum Ca^{2+}-ATPase, resulted in caspase-3 activation in both wild-type and mutant striatal cells (data not shown). These data indicate that mutant striatal cells have the capacity to die by apoptosis. Therefore it can be postulated that a deficit in mitochondrial complex II activity specifically switched the 3-NP-induced cell death in the mutant striatal cells from an apoptotic to a non–apoptotic form.

Given that mutant striatal cells died via a non-apoptotic process, the pronounced loss of $\Delta\psi m$ likely plays a significant role in the increased vulnerability of mutant striatal cells to 3-NP-induced toxicity. The decrease of $\Delta\psi m$ can be caused by the opening of the PTP (17). *In vitro*, rat brain mitochondria maintain both NAD(P)H reduction and $\Delta\psi m$ during continuous calcium loading until PTP opening (63). Indeed, CsA, a potent inhibitor of PTP opening protected the mutant striatal cells against the 3-NP-induced loss of $\Delta\psi m$ and cell death.

Mitochondrial calcium overload appears to be an essential factor in PTP opening (18). In a transgenic mouse model of HD there is data to suggest that the calcium buffering capacity of the neurons expressing mutant htt is impaired (64), and mitochondria from HD patients depolarize at lower calcium levels and exhibit a reduction in calcium retention capacity (29). Further, incubation of normal mitochondria with a Q62-GST fusion protein resulted in the mitochondria depolarizing at lower calcium concentrations than mitochondria incubated with GST alone or a Q19-GST fusion protein (30). PTP is composed of the adenine nucleotide translocase (ANT), cyclophilin D (a *cis–trans* proline isomerase), the voltage dependent anion channel (VDAC) and other proteins (18). Calcium binding to the ANT within the mitochondrial matrix results in a conformational change that is catalyzed in part by cyclophilin D resulting in PTP opening and subsequent loss of $\Delta\psi m$ (18). Therefore, mutant htt may sensitize striatal cells to 3-NP-induced cell death by directly or indirectly facilitating PTP opening, possibly by allowing calcium to bind the ANT at a lower concentration (18).

The fact that both inhibition of the calcium uniporter and PTP opening (18) effectively blocked 3-NP-induced cell death in the mutant cells strongly implicates calcium overload and PTP opening as key events in the cell death process. Ruthenium

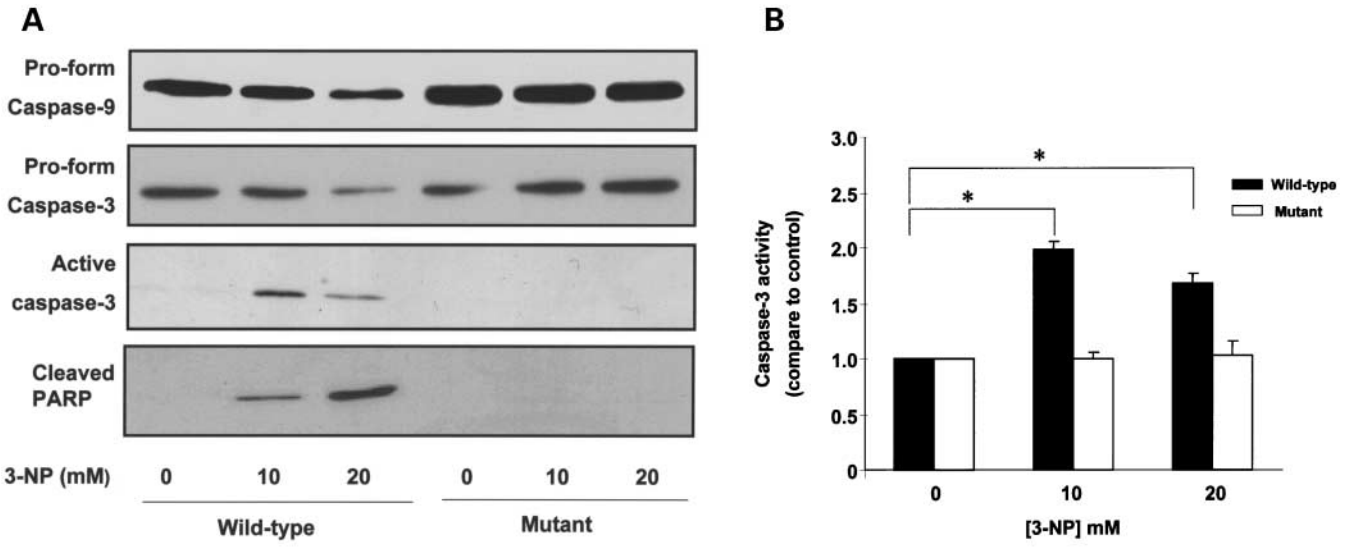

Figure 5. 3-NP treatment results in caspase-9, and caspase-3 activation, and PARP cleavage in wild-type striatal cells but not in mutant striatal cells. Cells were incubated under control conditions (0 mM 3-NP), or in the presence of 10 or 20 mM 3-NP for 40 h. (**A**) Samples were then immunoblotted for the pro-form of caspase-9, active caspase-3 or cleaved PARP. No active caspase-3 or cleaved PARP was detected in either cell line under control conditions. After 3-NP treatment, active caspase-3 and cleaved PARP was present in wild-type striatal cells but not in mutant striatal cells. In the wild-type striatal cells, treatment with 3-NP resulted in a decrease in the levels of the pro-form of caspase-9, indicating that caspase-9 is cleaved and activated. In mutant striatal cells, no change in the levels of the pro-form of caspase-9 was detected in response to 3-NP treatment. Immunoblots shown are representative of three to six independent experiments. (**B**) 3-NP treatment led to a significant increase of caspase-3 activity in wild-type striatal cells, but not in mutant striatal cells. Results are expressed as a percent of caspase-3 activity in cells under control conditions. Mean ± SEM. $n = 3$. $^*P < 0.05$ when compared with cells under control conditions.

red also restored the $\Delta\psi$m in mutant striatal cells treated with 3-NP, further substantiating the hypothesis that abnormalities in calcium handling sensitize mutant striatal cells to 3-NP-induced toxicity through a mechanism involving mitochondrial membrane depolarization.

Intriguingly, mitochondria isolated from striatum are more sensitive to calcium-induced PTP opening than cortical mitochondria (65), differences that may contribute to the selective cell death of striatal neurons that occurs in HD. The 3-NP-induced cell death of wild-type striatal cells did not involve PTP opening, as inhibitor of PTP by CsA, did not prevent cell death. It should also be noted that in another study CsA did not protect against 3-NP-induced cell death in rat neuronal RN33B cells (66), demonstrating that the cell death may be independent of PTP opening. Since in wild-type striatal cells, ruthenium red, an inhibitor of calcium influx, only modestly decreased 3-NP-induced cell death, this would suggest that a moderate mitochondrial calcium influx might contribute to this cell death, although to a significantly lesser extent than that in mutant striatal cells.

There have been debates about whether release of cytochrome c is through the opening of PTP and subsequent mitochondrial membrane depolarization. Although some studies show that opening of PTP is an essential component in the signaling pathway for cytochrome c release (67), there is also data demonstrating that release of cytochrome c does not necessarily require PTP opening (68). Intriguingly, in isolated liver mitochondria calcium-induced PTP opening is essential for cytochrome c release, however in brain mitochondria cytochrome c is released through a mechanism that does not require PTP opening (69). In agreement with these findings, we found that cytochrome c release and PTP opening are two independent processes in striatal cells. In mutant striatal cells, although 3-NP treatment resulted in PTP opening, no cytochrome c release was observed. In contrast, in wild-type striatal cells 3-NP treatment resulted in a significant amount of cytochrome c being released to the cytosol, with only a minimal loss of $\Delta\psi$m. These data clearly demonstrate that loss of $\Delta\psi$m and the release of cytochrome c are not necessarily associated.

It is well established that ATP thresholds are an important factor in determining whether a cell will die by an apoptotic or non-apoptotic pathway (12). In the mutant striatal cells, ATP levels are lower than in the wild-type cells (33), and mitochondrial complex II activity and mitochondrial respiration using succinate as a substrate are significantly decreased in the mutant striatal cells compared with the wild-type cells (unpublished observations, T. Milakovic and G.V.W. Johnson). These data suggest that the presence of mutant htt affects the functioning of complex II. Therefore it can be speculated that the 3-NP treatment of the mutant striatal cells results in ATP levels that are below the threshold required for apoptosis and hence they 'abort' to a non-apoptotic program. However, ATP depletion alone is not the direct cause of the death of the mutant striatal cells in response to 3-NP, rather it is one variable that determines which cell death pathway will be taken. So what actually causes the enhanced non-apoptotic cell death in 3-NP treated striatal cells? It seems that the impaired ability of the mitochondria in cells expressing mutant htt to handle calcium is an essential factor in this process (29,30). Inhibition of calcium influx or inhibition of the PTP opening offered remarkable protection against 3-NP-induced cell death in the

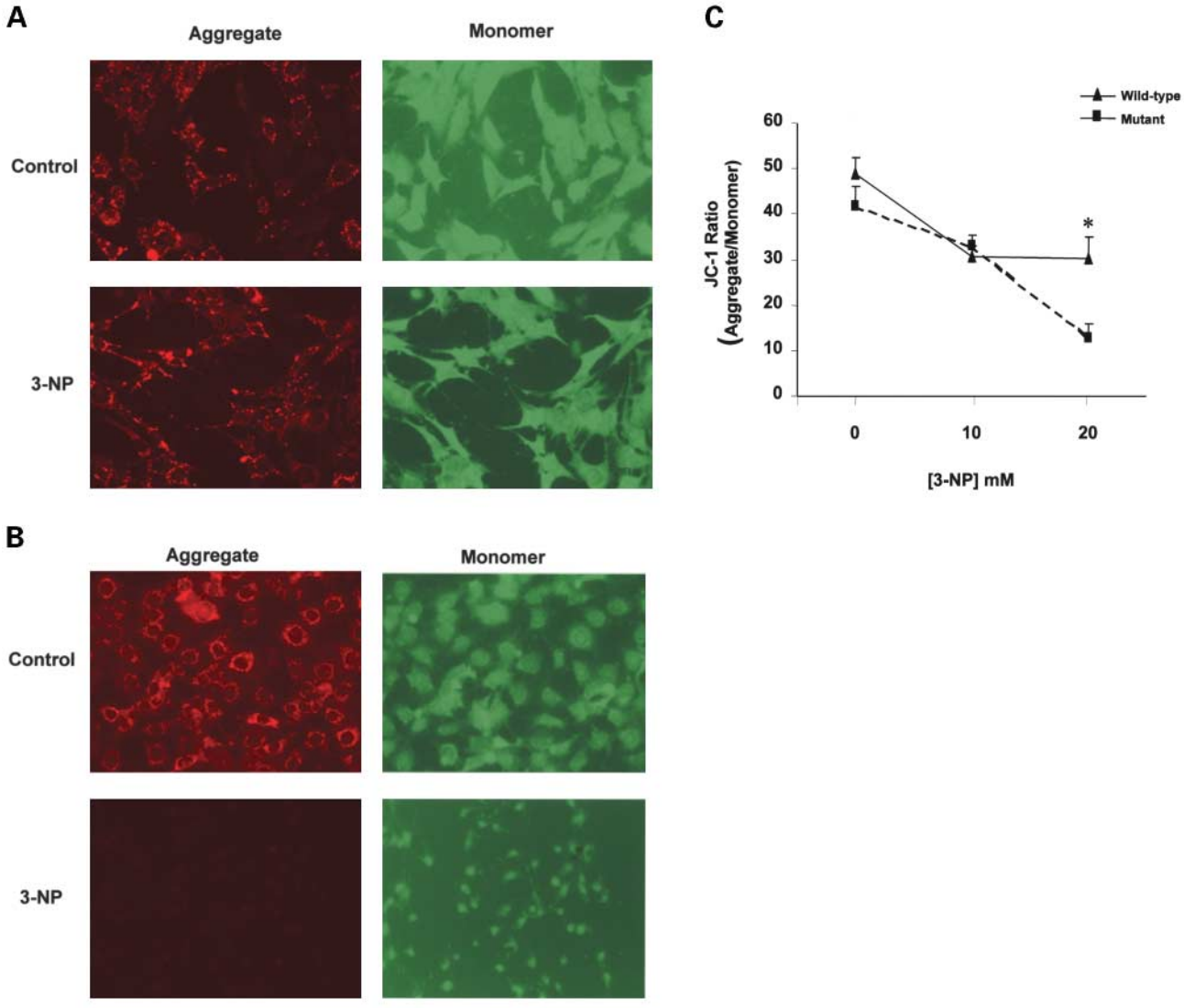

Figure 6. 3-NP treatment results in a greater decrease of $\Delta\psi m$ in mutant striatal cells than in wild-type striatal cells. Wild-type or mutant striatal cells were incubated under control conditions, or in the presence of 3-NP for 40 h, and subsequently incubated with the mitochondrial membrane potential-sensitive dye JC-1 then viewed with a Nikon Diaphot or quantitated with fluorescence plate reader. (**A**, **B**) Images showing that mutant striatal cells lose $\Delta\psi m$ to a significantly greater extent than wild-type striatal cells in response to 10 mM 3-NP. In control conditions both wild-type (A) and mutant (B) striatal cells exhibit red JC-1 aggregates, indicative of a relatively high $\Delta\psi m$. In the wild-type striatal cells (A) treatment with 3-NP did not noticeably reduce the presence of the red JC-1 aggregates. In contrast, treatment of the mutant striatal cells (B) with 3-NP resulted in a dramatic decrease in the presence of red JC-1 aggregates, indicating that the mitochondrial membrane was highly depolarized. (**C**) Quantitated data also showing that mutant striatal cells (dashed line) lose $\Delta\psi m$ to a significantly greater extent than wild-type striatal cells (solid line) in response to 20 mM 3-NP. The ratio was obtained by dividing JC-1 aggregate fluorescence by monomer fluorescence. Mean $\pm$ SEM, $n = 3$, $^*P < 0.05$ when comparing the values between cell lines.

mutant striatal cells, clearly demonstrating the importance of calcium overload and PTP opening in the death cascade. Therefore it is likely that the combination of impaired complex II activity and the associated decrease in ATP production, and impaired calcium handling by the mitochondria may increase the sensitivity of mutant striatal cells to 3-NP toxicity resulting in non-apoptotic cell death.

In conclusion, these studies show that mutant htt specifically increases cell vulnerability to mitochondrial complex II inhibition. Further, the presence of mutant htt 'switches' the type of cell death from predominantly a controlled apoptotic process to a non-apoptotic process involving mitochondrial calcium overload followed by opening of the PTP, resulting in loss of mitochondrial membrane potential.

MATERIALS AND METHODS

Materials

3-NP (Sigma, St Louis, MO, USA) was dissolved in distilled water and neutralized to pH 7.4 with NaOH, and it was freshly prepared each time before treatment. Ruthenium red (Sigma, St Louis, MO, USA) was prepared as a 1000× stock in distilled

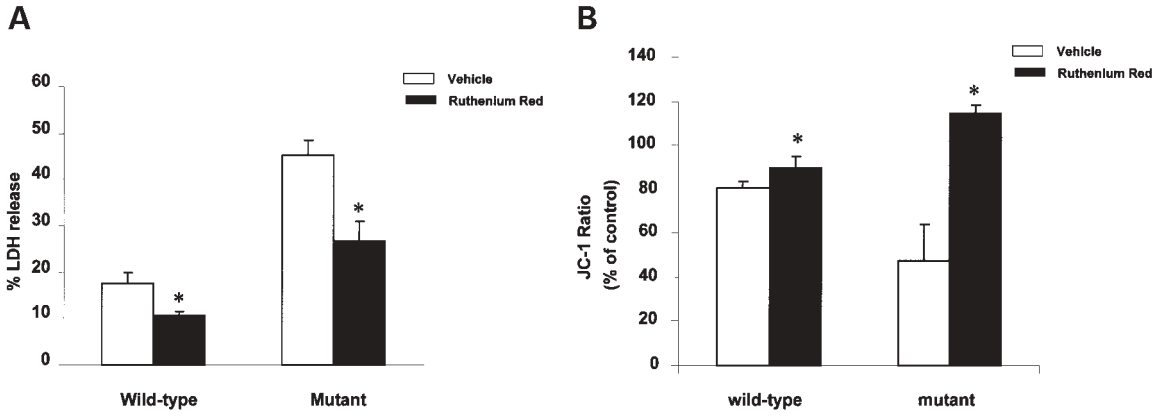

Figure 7. Ruthenium red reduces 3-NP-induced cell death in mutant and wild-type striatal cells. Wild-type and mutant striatal cells were treated with 20 mM 3-NP for 40 h with (ruthenium red) or without (vehicle) 1 μM ruthenium red. (**A**) Ruthenium red significantly decreased cell death in 3-NP treated mutant and wild-type striatal cells. Cell death was measured by LDH release. $*P < 0.05$ when comparing cell death with cells treated with 3-NP only. Mean ± SEM, $n = 3$. (**B**) Ruthenium red inhibited the 3-NP-induced $\Delta\psi$m decrease in mutant striatal cells and wild-type striatal cells. Data are presented as a percent of control (untreated) values. Mean ± SEM, $n = 3$, $*P < 0.05$, when comparing the JC-1 ratio with cells treated with 3-NP only.

water. Rotenone (Sigma, St Louis, MO, USA), CsA (Alexis, San Diego, CA, USA) and BAF (Alexis, San Diego, CA, USA) were prepared as 1000× stocks in dimethyl sulfoxide. When applied, ruthenium red, CsA or BAF was added 1 h prior to 3-NP treatment and re-added 20 h after the initiation of 3-NP treatment. All treatments were carried out in serum free media.

Cell culture

STHdh$^{Q7/Q7}$ and STHdh$^{Q111/Q111}$ cells. Conditionally immortalized wild-type ST*Hdh*$^{Q7/Q7}$ striatal neuronal progenitor cells expressing endogenous normal htt (referred to as wild-type striatal cells), and homozygous mutant ST*Hdh*$^{Q111/Q111}$ striatal neuronal progenitor cell lines from homozygous *Hdh*$^{Q111/Q111}$ knock-in mice expressing mutant htt with 111 glutamines (referred to as mutant striatal cells), were described previously (31). The striatal cell lines were cultured at 33°C in Dulbecco's modified Eagle's medium (DMEM, Gibco, Gaithersburg, MD, USA) supplemented with 8% fetal bovine serum (Hyclone, Logan, UT, USA), 10 U/ml penicillin (Gibco, Gaithersburg, MD, USA), 100 μg/ml streptomycin (Gibco, Gaithersburg, MD, USA), and 2 mM L-glutamine (Gibco, Gaithersburg, MD, USA). Cells were grown in a humidified atmosphere containing 5% CO_2.

FL-Q23 and FL-Q82 cells. Human SH-SY5Y neuroblastoma cell lines stably expressing full-length htt with 23 (FL-Q23) or 82 (FL-Q82) glutamine repeats have been described previously (70). FL-Q23 and FL-Q82 cells were selected based on their resistance to G418, subcloned and maintained in RPMI 1640 medium (Gibco, Gaithersburg, MD, USA) supplemented with 2 mM L-glutamine, 10 U/ml penicillin, 100 μg/ml streptomycin, 5% fetal clone II serum (Hyclone, Logan, UT, USA), 10% horse serum (Gibco, Gaithersburg, MD, USA), and 100 μg/ml G418 (Gibco, Gaithersburg, MD, USA). Cells were grown in a humidified atmosphere containing 5% CO_2 at 37°C.

Cell viability measures

LDH assay. The release of the intracellular enzyme lactate dehydrogenase (LDH) into the medium was used as a quantitative measurement of cell viability. The measurement of LDH was carried out as described previously (71).

Live cell assay. In some experiments, cell viability was determined by using the calcein-AM (Molecular Probes Inc., Eugene, OR, USA). Non-fluorescent calcein-AM is converted into green fluorescent calcein by intracellular esterases and indicates the presence of active cell metabolism (72,73). It is a well-established method and has been used to measure cell viability in neuronal cell models (74). In each well of a 24 well plate 1.5×10^5 cells were plated. After treatment, the cells were incubated with calcein-AM (final concentration of 1 μM) for 30 min at room temperature and the fluorescence was measured on a fluorescence plate reader (Bio-Tek, Winooski, VT, USA) set at 485 nm excitation and 528 nm emission. Cell viability was expressed as a percentage of the signal obtained from the cells exposed to vehicle only.

Cell counting. Cell number was determined as described previously (33). In brief, cells were plated on four-chambered Lab-Tek glass slides (Nalge-Nunc International, Rochester, NY, USA). After treatment, cells were fixed with 4% paraformaldehyde and incubated with 4′,6-diamidino-2-phenylindole (DAPI; Molecular Probes, Eugene, OR, USA). DAPI-stained nuclei were counted using a Nikon Diaphot 200 epifluorescence microscope. Data were expressed as the proportion of nuclei counted in treated wells relative to nuclei counted in parallel untreated wells.

Apoptotic chromatin condensation determination

Cells were plated on glass coverslips coated with poly-D-lysine in Costar six-well dishes. After treatment, cells were rinsed

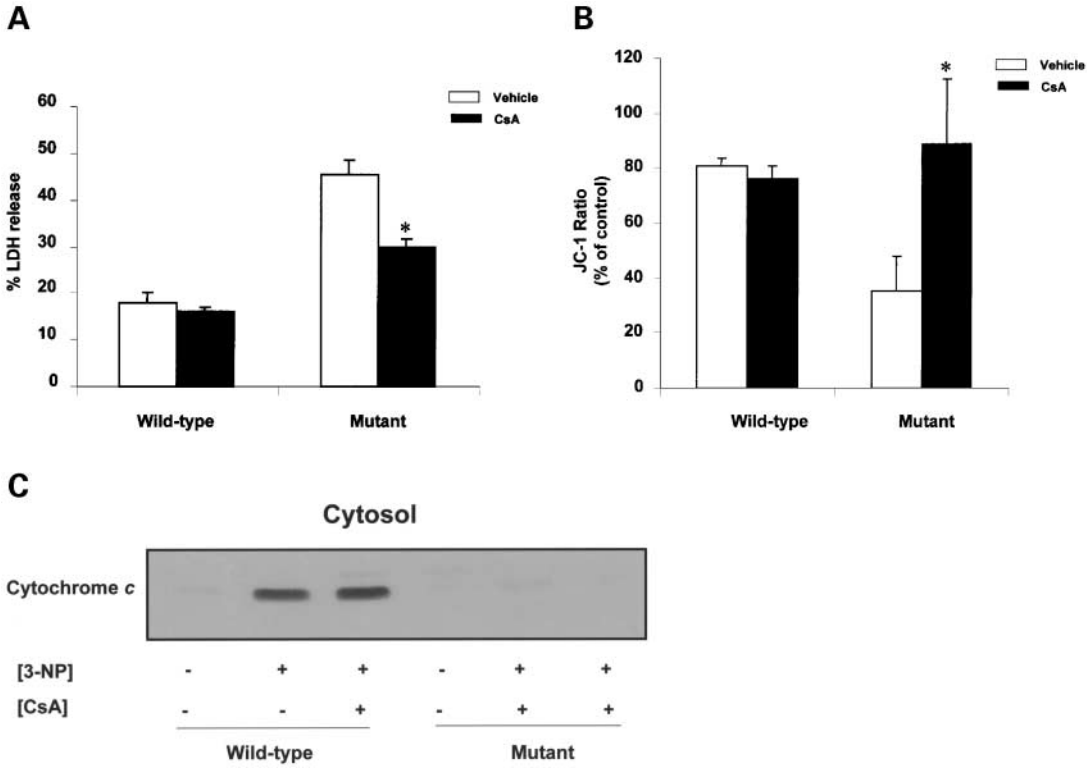

Figure 8. Effect of CsA on 3-NP-induced cell death in wild-type and mutant striatal cells. Wild-type and mutant striatal cells were treated with 20 mM 3-NP for 40 h with (CsA) or without (vehicle) 2 μM CsA. (**A**) CsA inhibited 3-NP-induced cell death in wild-type but not mutant striatal cells. Cell death was measured by LDH release. $*P < 0.05$, when comparing cell death with cells treated with 3-NP only. Mean ± SEM, $n = 3$. (**B**) CsA inhibited the 3-NP-induced $\Delta\psi m$ decrease in mutant striatal cells but not wild-type striatal cells. Data are presented as a percent of control (untreated) values. Mean ± SEM, $n = 3$, $*P < 0.05$, when comparing the JC-1 ratio with cells treated with 3-NP only. (**C**) CsA did not inhibit 3-NP-induced cytochrome c release in wild-type striatal cells. Cytosolic fractions were isolated and were probed for cytochrome c after incubation in the presence or absence of 3-NP and presence or absence of CsA. In the wild-type striatal cells, CsA co-treatment did not prevent cytochrome c release induced by 3-NP treatment, while in mutant striatal cells no cytosolic cytochrome c was detected under any condition. Immunoblots shown are representative of three to six independent experiments.

once with phosphate-buffered saline (PBS) and fixed with 4% paraformaldehyde at room temperature for 30 min. After fixation, cells were rinsed three times with PBS and incubated with 5 μg/ml DAPI for 10 min at room temperature in the dark. Cells were rinsed three times with PBS and once with sterile H_2O before mounting upside-down onto a glass microscope slide with immuno-mount (Thermo Shandon, Pittsburgh, PA, USA). Nuclei were visualized using a Nikon Diaphot 200 epifluorescence microscope and a Digital Spot camera (Diagnostic Instruments Inc., Sterling Heights, MI, USA) was used to capture images which were digitally stored and displayed using accompanying software.

Immunoblotting

Cells were rinsed in ice-cold PBS and collected in lysis buffer, containing 0.5% NP-40, 150 mM NaCl, 10 mM Tris–Cl (pH 7.4), 1 mM EGTA, 1 mM EDTA, 0.1 mM phenylmethylsulfonyl fluoride, 1 μM okadaic acid, and 10 μg/ml each of aprotinin, leupeptin, and pepstatin. Samples were sonicated on ice for 10 s and centrifuged at 16 000*g* for 10 min. Protein concentrations of supernatants were then determined by the bicinchoninic acid assay (BCA; Pierce, Rockford, IL, USA) and samples were diluted to a final concentration of 1 mg/ml with 2× reducing stop buffer (0.25 M Tris–HCl, pH 6.8, 5 mM EDTA, 5 mM EGTA, 25 mM dithiothreitol, 2% SDS, 10% glycerol and bromophenol blue as the tracking dye). Samples (20 μg of protein) were resolved on 10 or 12.5% SDS-polyacrylamide gels and transferred to nitrocellulose. Blots were blocked in 5% non-fat dry milk in TBST (20 mM Tris–HCl, pH 7.6, 137 mM NaCl, 0.05% Tween 20) for 1 h at room temperature. The blots were then incubated with an anti-cleaved caspase-3 polyclonal antibody (Cell Signaling, Beverly, MA, USA), anti-caspase-9 (Cell Signaling, Beverly, MA, USA), or with the anti-cleaved PARP polyclonal antibody (Cell Signaling, Beverly, MA, USA) in the same buffer overnight at 4°C. The membranes were then washed three times with TBST and incubated with HRP-conjugated secondary antibody for 2 h at room temperature. The membranes were rinsed three times for 30 min with TBST, followed by four quick rinses with distilled water, and developed with the enhanced chemiluminescence method (ECL; Amersham Pharmacia Biotech, UK).

Subcellular fractionation

Cells were rinsed in ice-cold PBS and collected in cavitation buffer (3 mM $MgCl_2$, 250 mM sucrose, 1 mM EGTA, and 5 mM HEPES, pH 7.4) supplemented with 0.1 mM phenylmethylsulfonyl

fluoride, 1 μM okadaic acid, and 10 μg/ml each of aprotinin, leupeptin and pepstatin. Cells were then disrupted by N_2 cavitation for 5 min at 250 psi on ice, and the resulting cell lysate was centrifuged at 350*g* for 5 min at 4°C to eliminate nuclei, large debris and unbroken cells. The resulting supernatant was then centrifuged at 10 000*g* for 10 min at 4°C to obtain the heavy membrane pellet enriched for mitochondria, and the resulting supernatant was centrifuged at 100 000*g* for 1 h to remove any cellular debris and was used as the cytosolic fraction.

In situ caspase-3 activity

In situ caspase-3 activity was measured using a previously described protocol (75). In brief, 200 μl of assay buffer (20 mM Hepes, pH 7.5, 10% glycerol, and 2 mM dithiothreitol) containing the peptide substrate for caspase-3 (AC-DEVD-AMC) was added to each well (final concentration of 25 ng/μl) of a 96-well clear bottom plate (Corning). Cell lysate (20 μg of protein) was added to start the reaction. Triplicate measurements were done for each sample. Background fluorescence was measured in wells containing assay buffer, substrate, and lysis buffer without the cell lysate. Assay plates were incubated at 37°C for 1 h, and fluorescence was measured on a fluorescence plate reader set at 360 nm excitation and 460 nm emission.

Detection of the mitochondrial membrane potential (Δψm)

Δψm was analyzed using 5,5′,6,6′-tetrachloro-1,1′,3,3-tetraethylbenzimidazolyl-carbocyanine iodide (JC-1; Molecular Probes, Eugene, OR, USA) a lipophilic cationic fluorescence dye. JC-1 is driven into mitochondria in a membrane potential-dependent manner. At high mitochondrial membrane potentials, JC-1 accumulates sufficiently in the mitochondria to form aggregates that fluoresce red. At lower mitochondrial potentials, less dye enters mitochondria resulting in monomers that fluoresce green (76,77). For these studies cells were grown on 24-well plates. After treatment, cells were incubated with 5 μg/ml JC-1 (made up as a 1 mg/ml stock in dimethyl sulfoxide) for 30 min at room temperature in the dark. Then cells were washed twice with PBS and fluorescence was measured on a fluorescence plate reader set at 485 nm excitation and 528 nm emission for green monomer or 530 nm excitation and 590 nm emission for red aggregate. Cells were also monitored with a Nikon Diaphot and images were captured with a Digital Spot camera using the same exposure time for all fields and displayed with its accompanying software.

Statistic analysis

Data were analyzed using Student's *t*-test. Values were considered significantly different when the two-tailed *P*-value was <0.05. Results are expressed as means ± SEM.

ACKNOWLEDGEMENTS

This work was supported by NIH grants NS41744 (G.V.W.J.) and NS16367 and NS32765 (M.E.M.).

REFERENCES

1. Vonsattel, J.P. and DiFiglia, M. (1998) Huntington disease. *J. Neuropathol. Exp. Neurol.*, **57**, 369–384.
2. The Huntington's Disease Collaborative Research Group (1993) A novel gene containing a trinucleotide repeat that is expanded and unstable on Huntington's disease chromosomes. *Cell*, **72**, 971–983.
3. Gutekunst, C.A., Levey, A.I., Heilman, C.J., Whaley, W.L., Yi, H., Nash, N.R., Rees, H.D., Madden, J.J. and Hersch, S.M. (1995) Identification and localization of huntingtin in brain and human lymphoblastoid cell lines with anti-fusion protein antibodies. *Proc. Natl Acad. Sci. USA*, **92**, 8710–8714.
4. Strong, T.V., Tagle, D.A., Valdes, J.M., Elmer, L.W., Boehm, K., Swaroop, M., Kaatz, K.W., Collins, F.S. and Albin, R.L. (1993) Widespread expression of the human and rat Huntington's disease gene in brain and nonneural tissues. *Nat. Genet.*, **5**, 259–265.
5. Vonsattel, J.P., Myers, R.H., Stevens, T.J., Ferrante, R.J., Bird, E.D. and Richardson, E.P. Jr (1985) Neuropathological classification of Huntington's disease. *J. Neuropathol. Exp. Neurol.*, **44**, 559–577.
6. Kiechle, T., Dedeoglu, A., Kubilus, J., Kowall, N.W., Beal, M.F., Friedlander, R.M., Hersch, S.M. and Ferrante, R.J. (2002) Cytochrome C and caspase-9 expression in Huntington's disease. *Neuromol. Med.*, **1**, 183–195.
7. Ona, V.O., Li, M., Vonsattel, J.P., Andrews, L.J., Khan, S.Q., Chung, W.M., Frey, A.S., Menon, A.S., Li, X.J., Stieg, P.E. *et al.* (1999) Inhibition of caspase-1 slows disease progression in a mouse model of Huntington's disease. *Nature*, **399**, 263–267.
8. Chen, M., Ona, V.O., Li, M., Ferrante, R.J., Fink, K.B., Zhu, S., Bian, J., Guo, L., Farrell, L.A., Hersch, S.M. *et al.* (2000) Minocycline inhibits caspase-1 and caspase-3 expression and delays mortality in a transgenic mouse model of Huntington disease. *Nat. Med.*, **6**, 797–801.
9. Wheeler, V.C., Gutekunst, C.A., Vrbanac, V., Lebel, L.A., Schilling, G., Hersch, S., Friedlander, R.M., Gusella, J.F., Vonsattel, J.P., Borchelt, D.R. *et al.* (2002) Early phenotypes that presage late-onset neurodegenerative disease allow testing of modifiers in Hdh CAG knock-in mice. *Hum. Mol. Genet.*, **11**, 633–640.
10. Lin, C.H., Tallaksen-Greene, S., Chien, W.M., Cearley, J.A., Jackson, W.S., Crouse, A.B., Ren, S., Li, X.J., Albin, R.L. and Detloff, P.J. (2001) Neurological abnormalities in a knock-in mouse model of Huntington's disease. *Hum. Mol. Genet.*, **10**, 137–144.
11. Menalled, L.B., Sison, J.D., Wu, Y., Olivieri, M., Li, X.J., Li, H., Zeitlin, S. and Chesselet, M.F. (2002) Early motor dysfunction and striosomal distribution of huntingtin microaggregates in Huntington's disease knock-in mice. *J. Neurosci.*, **22**, 8266–8276.
12. Kroemer, G. and Reed, J.C. (2000) Mitochondrial control of cell death. *Nat. Med.*, **6**, 513–519.
13. Li, P., Nijhawan, D., Budihardjo, I., Srinivasula, S.M., Ahmad, M., Alnemri, E.S. and Wang, X. (1997) Cytochrome c and dATP-dependent formation of Apaf-1/caspase-9 complex initiates an apoptotic protease cascade. *Cell*, **91**, 479–489.
14. Shi, Y. (2002) Mechanisms of caspase activation and inhibition during apoptosis. *Mol. Cell*, **9**, 459–470.
15. Hengartner, M.O. (2000) The biochemistry of apoptosis. *Nature*, **407**, 770–776.
16. Tong, W.M., Ohgaki, H., Huang, H., Granier, C., Kleihues, P. and Wang, Z.Q. (2003) Null mutation of DNA strand break-binding molecule poly(ADP-ribose) polymerase causes medulloblastomas in p53(−/−) mice. *Am. J. Pathol.*, **162**, 343–352.
17. Kim, J.S., He, L. and Lemasters, J.J. (2003) Mitochondrial permeability transition: a common pathway to necrosis and apoptosis. *Biochem. Biophys. Res. Commun.*, **304**, 463–470.
18. Halestrap, A.P., McStay, G.P. and Clarke, S.J. (2002) The permeability transition pore complex: another view. *Biochimie*, **84**, 153–166.
19. Tafani, M., Schneider, T.G., Pastorino, J.G. and Farber, J.L. (2000) Cytochrome c-dependent activation of caspase-3 by tumor necrosis factor requires induction of the mitochondrial permeability transition. *Am. J. Pathol.*, **156**, 2111–2121.
20. Brustovetsky, N., Jemmerson, R. and Dubinsky, J.M. (2002) Calcium-induced Cytochrome c release from rat brain mitochondria is altered by digitonin. *Neurosci. Lett.*, **332**, 91–94.
21. Niquet, J., Baldwin, R.A., Allen, S.G., Fujikawa, D.G. and Wasterlain, C.G. (2003) Hypoxic neuronal necrosis: protein synthesis-independent activation of a cell death program. *Proc. Natl Acad. Sci. USA*, **100**, 2825–2830.

22. Tabrizi, S.J., Cleeter, M.W., Xuereb, J., Taanman, J.W., Cooper, J.M. and Schapira, A.H. (1999) Biochemical abnormalities and excitotoxicity in Huntington's disease brain. *Ann. Neurol.*, **45**, 25–32.
23. Sawa, A., Wiegand, G.W., Cooper, J., Margolis, R.L., Sharp, A.H., Lawler, J.F. Jr. Greenamyre, J.T., Snyder, S.H. and Ross, C.A. (1999) Increased apoptosis of Huntington disease lymphoblasts associated with repeat length-dependent mitochondrial depolarization. *Nat. Med.*, **5**, 1194–1198.
24. Gu, M., Gash, M.T., Mann, V.M., Javoy-Agid, F., Cooper, J.M. and Schapira, A.H. (1996) Mitochondrial defect in Huntington's disease caudate nucleus. *Ann. Neurol.*, **39**, 385–389.
25. Browne, S.E., Bowling, A.C., MacGarvey, U., Baik, M.J., Berger, S.C., Muqit, M.M., Bird, E.D. and Beal, M.F. (1997) Oxidative damage and metabolic dysfunction in Huntington's disease: selective vulnerability of the basal ganglia. *Ann. Neurol.*, **41**, 646–653.
26. Brouillet, E., Hantraye, P., Ferrante, R.J., Dolan, R., Leroy-Willig, A., Kowall, N.W. and Beal, M.F. (1995) Chronic mitochondrial energy impairment produces selective striatal degeneration and abnormal choreiform movements in primates. *Proc. Natl Acad. Sci. USA*, **92**, 7105–7109.
27. Brouillet, E. and Hantraye, P. (1995) Effects of chronic MPTP and 3-nitropropionic acid in nonhuman primates. *Curr. Opin. Neurol.*, **8**, 469–473.
28. Beal, M.F., Brouillet, E., Jenkins, B.G., Ferrante, R.J., Kowall, N.W., Miller, J.M., Storey, E., Srivastava, R., Rosen, B.R. and Hyman, B.T. (1993) Neurochemical and histologic characterization of striatal excitotoxic lesions produced by the mitochondrial toxin 3-nitropropionic acid. *J. Neurosci.*, **13**, 4181–4192.
29. Panov, A.V., Gutekunst, C.A., Leavitt, B.R., Hayden, M.R., Burke, J.R., Strittmatter, W.J. and Greenamyre, J.T. (2002) Early mitochondrial calcium defects in Huntington's disease are a direct effect of polyglutamines. *Nat. Neurosci.*, **5**, 731–736.
30. Panov, A.V., Burke, J.R., Strittmatter, W.J. and Greenamyre, J.T. (2003) *In vitro* effects of polyglutamine tracts on Ca^{2+}-dependent depolarization of rat and human mitochondria: relevance to Huntington's disease. *Arch. Biochem. Biophys.*, **410**, 1–6.
31. Trettel, F., Rigamonti, D., Hilditch-Maguire, P., Wheeler, V.C., Sharp, A.H., Persichetti, F., Cattaneo, E. and MacDonald, M.E. (2000) Dominant phenotypes produced by the HD mutation in STHdh(Q111) striatal cells. *Hum. Mol. Genet.*, **9**, 2799–2809.
32. Ludolph, A.C., He, F., Spencer, P.S., Hammerstad, J. and Sabri, M. (1991) 3-Nitropropionic acid-exogenous animal neurotoxin and possible human striatal toxin. *Can. J. Neurol. Sci.*, **18**, 492–498.
33. Gines, S., Seong, I.S., Fossale, E., Ivanova, E., Trettel, F., Gusella, J.F., Wheeler, V.C., Persichetti, F. and MacDonald, M.E. (2003) Specific progressive cAMP reduction implicates energy deficit in presymptomatic Huntington's disease knock-in mice. *Hum. Mol. Genet.*, **12**, 497–508.
34. Bernas, T. and Dobrucki, J. (2002) Mitochondrial and nonmitochondrial reduction of MTT: interaction of MTT with TMRE, JC-1, and NAO mitochondrial fluorescent probes. *Cytometry*, **47**, 236–242.
35. Petersen, A., Larsen, K.E., Behr, G.G., Romero, N., Przedborski, S., Brundin, P. and Sulzer, D. (2001) Expanded CAG repeats in exon 1 of the Huntington's disease gene stimulate dopamine-mediated striatal neuron autophagy and degeneration. *Hum. Mol. Genet.*, **10**, 1243–1254.
36. Kegel, K.B., Kim, M., Sapp, E., McIntyre, C., Castano, J.G., Aronin, N. and DiFiglia, M. (2000) Huntingtin expression stimulates endosomal–lysosomal activity, endosome tubulation, and autophagy. *J. Neurosci.*, **20**, 7268–7278.
37. Liu, X., Kim, C.N., Yang, J., Jemmerson, R. and Wang, X. (1996) Induction of apoptotic program in cell-free extracts: requirement for dATP and cytochrome c. *Cell*, **86**, 147–157.
38. Li, R., Bounds, D.J., Granville, D., Ip, S.H., Jiang, H., Margaron, P. and Hunt, D.W. (2003) Rapid induction of apoptosis in human keratinocytes with the photosensitizer QLT0074 via a direct mitochondrial action. *Apoptosis*, **8**, 269–275.
39. Lazebnik, Y.A., Kaufmann, S.H., Desnoyers, S., Poirier, G.G. and Earnshaw, W.C. (1994) Cleavage of poly(ADP-ribose) polymerase by a proteinase with properties like ICE. *Nature*, **371**, 346–347.
40. Deshmukh, M., Vasilakos, J., Deckwerth, T.L., Lampe, P.A., Shivers, B.D. and Johnson, E.M., Jr. (1996) Genetic and metabolic status of NGF-deprived sympathetic neurons saved by an inhibitor of ICE family proteases. *J. Cell Biol.*, **135**, 1341–1354.
41. Recchioni, R., Marcheselli, F., Moroni, F. and Pieri, C. (2002) Apoptosis in human aortic endothelial cells induced by hyperglycemic condition involves mitochondrial depolarization and is prevented by *N*-acetyl-L-cysteine. *Metabolism*, **51**, 1384–1388.
42. Kong, C.W., Hsu, T.G., Lu, F.J., Chan, W.L. and Tsai, K. (2001) Leukocyte mitochondria depolarization and apoptosis in advanced heart failure: clinical correlations and effect of therapy. *J. Am. Coll. Cardiol.*, **38**, 1693–1700.
43. Chang, L.K. and Johnson, E.M. Jr (2002) Cyclosporin A inhibits caspase-independent death of NGF-deprived sympathetic neurons: a potential role for mitochondrial permeability transition. *J. Cell Biol.*, **157**, 771–781.
44. Deckel, A.W., Elder, R. and Fuhrer, G. (2002) Biphasic developmental changes in Ca^{2+}/calmodulin-dependent proteins in R6/2 Huntington's disease mice. *Neuroreport*, **13**, 707–711.
45. Hansson, O., Guatteo, E., Mercuri, N.B., Bernardi, G., Li, X.J., Castilho, R.F. and Brundin, P. (2001) Resistance to NMDA toxicity correlates with appearance of nuclear inclusions, behavioural deficits and changes in calcium homeostasis in mice transgenic for exon 1 of the huntington gene. *Eur. J. Neurosci.*, **14**, 1492–1504.
46. Kruman, II and Mattson, M.P. (1999) Pivotal role of mitochondrial calcium uptake in neural cell apoptosis and necrosis. *J. Neurochem.*, **72**, 529–540.
47. Gunter, T.E., Buntinas, L., Sparagna, G., Eliseev, R. and Gunter, K. (2000) Mitochondrial calcium transport: mechanisms and functions. *Cell Calcium*, **28**, 285–296.
48. Ly, J.D., Grubb, D.R. and Lawen, A. (2003) The mitochondrial membrane potential (Deltapsi(m)) in apoptosis; an update. *Apoptosis*, **8**, 115–128.
49. Hansson, M.J., Persson, T., Friberg, H., Keep, M.F., Rees, A., Wieloch, T. and Elmer, E. (2003) Powerful cyclosporin inhibition of calcium-induced permeability transition in brain mitochondria. *Brain Res.*, **960**, 99–111.
50. Hickey, M.A. and Morton, A.J. (2000) Mice transgenic for the Huntington's disease mutation are resistant to chronic 3-nitropropionic acid-induced striatal toxicity. *J. Neurochem.*, **75**, 2163–2171.
51. Bogdanov, M.B., Ferrante, R.J., Kuemmerle, S., Klivenyi, P. and Beal, M.F. (1998) Increased vulnerability to 3-nitropropionic acid in an animal model of Huntington's disease. *J. Neurochem.*, **71**, 2642–2644.
52. Mangiarini, L., Sathasivam, K., Seller, M., Cozens, B., Harper, A., Hetherington, C., Lawton, M., Trottier, Y., Lehrach, H., Davies, S.W. *et al.* (1996) Exon 1 of the HD gene with an expanded CAG repeat is sufficient to cause a progressive neurological phenotype in transgenic mice. *Cell*, **87**, 493–506.
53. Wheeler, V.C., White, J.K., Gutekunst, C.A., Vrbanac, V., Weaver, M., Li, X.J., Li, S.H., Yi, H., Vonsattel, J.P., Gusella, J.F. *et al.* (2000) Long glutamine tracts cause nuclear localization of a novel form of huntingtin in medium spiny striatal neurons in HdhQ92 and HdhQ111 knock-in mice. *Hum. Mol. Genet.*, **9**, 503–513.
54. Chan, E.Y., Luthi-Carter, R., Strand, A., Solano, S.M., Hanson, S.A., DeJohn, M.M., Kooperberg, C., Chase, K.O., DiFiglia, M., Young, A.B. *et al.* (2002) Increased huntingtin protein length reduces the number of polyglutamine-induced gene expression changes in mouse models of Huntington's disease. *Hum. Mol. Genet.*, **11**, 1939–1951.
55. Luthi-Carter, R., Strand, A., Peters, N.L., Solano, S.M., Hollingsworth, Z.R., Menon, A.S., Frey, A.S., Spektor, B.S., Penney, E.B., Schilling, G. *et al.* (2000) Decreased expression of striatal signaling genes in a mouse model of Huntington's disease. *Hum. Mol. Genet.*, **9**, 1259–1271.
56. Luthi-Carter, R., Hanson, S.A., Strand, A.D., Bergstrom, D.A., Chun, W., Peters, N.L., Woods, A.M., Chan, E.Y., Kooperberg, C., Krainc, D. *et al.* (2002) Dysregulation of gene expression in the R6/2 model of polyglutamine disease: parallel changes in muscle and brain. *Hum. Mol. Genet.*, **11**, 1911–1926.
57. Hagerhall, C. (1997) Succinate: quinone oxidoreductases. Variations on a conserved theme. *Biochim. Biophys. Acta*, **1320**, 107–141.
58. Pfanner, N. and Geissler, A. (2001) Versatility of the mitochondrial protein import machinery. *Nat. Rev. Mol. Cell Biol.*, **2**, 339–349.
59. Neupert, W. (1997) Protein import into mitochondria. *A. Rev. Biochem.*, **66**, 863–917.
60. Singaraja, R.R., Hadano, S., Metzler, M., Givan, S., Wellington, C.L., Warby, S., Yanai, A., Gutekunst, C.A., Leavitt, B.R., Yi, H. *et al.* (2002) HIP14, a novel ankyrin domain-containing protein, links huntingtin to intracellular trafficking and endocytosis. *Hum. Mol. Genet.*, **11**, 2815–2828.
61. Gutekunst, C.A., Li, S.H., Yi, H., Ferrante, R.J., Li, X.J. and Hersch, S.M. (1998) The cellular and subcellular localization of huntingtin-associated protein 1 (HAP1): comparison with huntingtin in rat and human. *J. Neurosci.*, **18**, 7674–7686.

62. Zhang, X., Chen, J., Graham, S.H., Du, L., Kochanek, P.M., Draviam, R., Guo, F., Nathaniel, P.D., Szabo, C., Watkins, S.C. *et al.* (2002) Intranuclear localization of apoptosis-inducing factor (AIF) and large scale DNA fragmentation after traumatic brain injury in rats and in neuronal cultures exposed to peroxynitrite. *J. Neurochem.*, **82**, 181–191.
63. Chalmers, S. and Nicholls, D.G. (2003) The relationship between free and total calcium concentrations in the matrix of liver and brain mitochondria. *J. Biol. Chem.*, **278**, 19062–19070.
64. Hodgson, J.G., Agopyan, N., Gutekunst, C.A., Leavitt, B.R., LePiane, F., Singaraja, R., Smith, D.J., Bissada, N., McCutcheon, K., Nasir, J. *et al.* (1999) A YAC mouse model for Huntington's disease with full-length mutant huntingtin, cytoplasmic toxicity, and selective striatal neurodegeneration. *Neuron*, **23**, 181–192.
65. Brustovetsky, N., Brustovetsky, T., Purl, K.J., Capano, M., Crompton, M. and Dubinsky, J.M. (2003) Increased susceptibility of striatal mitochondria to calcium-induced permeability transition. *J. Neurosci.*, **23**, 4858–4867.
66. Rodrigues, C.M., Stieers, C.L., Keene, C.D., Ma, X., Kren, B.T., Low, W.C. and Steer, C.J. (2000) Tauroursodeoxycholic acid partially prevents apoptosis induced by 3-nitropropionic acid: evidence for a mitochondrial pathway independent of the permeability transition. *J. Neurochem.*, **75**, 2368–2379.
67. Bradham, C.A., Qian, T., Streetz, K., Trautwein, C., Brenner, D.A. and Lemasters, J.J. (1998) The mitochondrial permeability transition is required for tumor necrosis factor alpha-mediated apoptosis and cytochrome c release. *Mol. Cell. Biol.*, **18**, 6353–6364.
68. Schild, L., Keilhoff, G., Augustin, W., Reiser, G. and Striggow, F. (2001) Distinct Ca^{2+} thresholds determine cytochrome c release or permeability transition pore opening in brain mitochondria. *FASEB J.*, **15**, 565–567.
69. Andreyev, A. and Fiskum, G. (1999) Calcium induced release of mitochondrial cytochrome c by different mechanisms selective for brain versus liver. *Cell Death Differ.*, **6**, 825–832.
70. Chun, W., Lesort, M., Tucholski, J., Faber, P.W., MacDonald, M.E., Ross, C.A. and Johnson, G.V. (2001) Tissue transglutaminase selectively modifies proteins associated with truncated mutant huntingtin in intact cells. *Neurobiol. Dis.*, **8**, 391–404.
71. Decker, T. and Lohmann-Matthes, M.L. (1988) A quick and simple method for the quantitation of lactate dehydrogenase release in measurements of cellular cytotoxicity and tumor necrosis factor (TNF) activity. *J. Immunol. Methods*, **115**, 61–69.
72. Gatti, R., Belletti, S., Orlandini, G., Bussolati, O., Dall'Asta, V. and Gazzola, G.C. (1998) Comparison of annexin V and calcein-AM as early vital markers of apoptosis in adherent cells by confocal laser microscopy. *J. Histochem. Cytochem.*, **46**, 895–900.
73. Rokhlin, O.W., Guseva, N., Tagiyev, A., Knudson, C.M. and Cohen, M.B. (2001) Bcl-2 oncoprotein protects the human prostatic carcinoma cell line PC3 from TRAIL-mediated apoptosis. *Oncogene*, **20**, 2836–2843.
74. Stout, A.K., Raphael, H.M., Kanterewicz, B.I., Klann, E. and Reynolds, I.J. (1998) Glutamate-induced neuron death requires mitochondrial calcium uptake. *Nat. Neurosci.*, **1**, 366–373.
75. Bijur, G.N., De Sarno, P. and Jope, R.S. (2000) Glycogen synthase kinase-3beta facilitates staurosporine- and heat shock-induced apoptosis. Protection by lithium. *J. Biol. Chem.*, **275**, 7583–7590.
76. Smiley, S.T., Reers, M., Mottola-Hartshorn, C., Lin, M., Chen, A., Smith, T.W., Steele, G.D. Jr and Chen, L.B. (1991) Intracellular heterogeneity in mitochondrial membrane potentials revealed by a J-aggregate-forming lipophilic cation JC-1. *Proc. Natl Acad. Sci. USA*, **88**, 3671–3675.
77. Nicholls, D.G. and Ward, M.W. (2000) Mitochondrial membrane potential and neuronal glutamate excitotoxicity: mortality and millivolts. *Trends Neurosci.*, **23**, 166–174.